Dynamic Behavior of Potential in the Plasma Core of the CHS Heliotron/Torsatron

A. Fujisawa,[1] H. Iguchi,[1] H. Sanuki,[1] K. Itoh,[1] S. Lee,[1] Y. Hamada,[1] S. Kubo,[1] H. Idei,[1] T. P. Crowley,[2] R. Akiyama,[1] K. Tanaka,[1] T. Minami,[1] K. Ida,[1] S. Nishimura,[1] S. Morita,[1] M. Kojima,[1] S. Hidekuma,[1] S.-I. Itoh,[3] C. Takahashi,[1] N. Inoue,[1] H. Suzuki,[1] S. Okamura,[1] and K. Matsuoka[1]

[1]*National Institute for Fusion Science Oroshi-cho, Toki-shi, Gifu, 509-52 Japan*

[2]*Rensselaer Polytechnic Institute, ECSE Department, Troy, New York 12180-3590*

[3]*RIAM, Kyushu University, Kasuga 816 Japan*

(Received 10 March 1997)

During combined electron cyclotron and neutral beam heating, an abrupt drop and rise in potential by about one half of the central electron temperature (~400 V) was observed in the core of the compact helical system heliotron/torsatron plasma. Drastic changes of radial electric field between positive and negative states occur over periods as short as 60 μs, which is much shorter than the energy confinement time scale of about a few milliseconds. A nonlinear relation between the radial electric field and radial current is obtained. This is the first experimental observation of a microsecond time scale spontaneous transition based on an electric field bifurcation in toroidal helical plasmas. [S0031-9007(97)03842-8]

PACS numbers: 52.55.Hc, 52.25.Fi, 52.35.Nx, 52.70.–m

Structural formation of the radial electric field in toroidal plasmas, such as tokamaks and stellarators, is a key physics issue associated with improved confinement modes, such as *H* mode [1,2]. It has been postulated that the origin of the *L*-*H* mode transition should be ascribed to a change in the structure of the radial electric field near the plasma edge [3,4]. A nonlinear dependence of plasma confinement on radial electric field should cause a bifurcation into two quite different states of better and worse confinement [5].

For toroidal helical plasmas, an absolute value of radial electric field is intrinsically influential to the confinement, since the helical ripple induced transport and loss cone loss are sensitive to the structure of the radial electric field. Neoclassical analysis has already shown that toroidal helical plasmas bifurcate into two states and possess the possibility of the existence of a solitary wave in the radial electric field [6,7]. This nonlinearity inherent in toroidal helical plasmas gives rise to dynamic and drastic behavior in the radial electric field. The formation mechanism of the radial electric field, therefore, is essentially governed by nonlinearity which is one of the main subjects of modern physics.

Heavy ion beam probe (HIBP) is a diagnostic to directly measure the internal plasma potential [8–10] with a high temporal and spatial resolution. A 200 keV HIBP [11,12] is installed on the Compact Helical System (CHS). CHS is a heliotron/torsatron device of medium size; its major and averaged minor radii are 1.0 and 0.2 m, respectively, and its periodicity is toroidally 8, and poloidally 2 [13]. In the first results with the HIBP, the steady state potential profiles exhibited widely varying characteristics for electron cyclotron heating (ECH) and neutral beam injection (NBI) plasmas [14].

In other earlier CHS experiments, charge exchange recombination spectroscopic (CXS) measurements were performed with a temporal resolution of about 17 ms. A change of electric field at ρ $(= r/a) \simeq 0.8$, from negative to positive, was observed, when an extra electron flux was induced with the use of ECH local heating [15,16]. However, the temporal resolution was too long to identify the transition nature of the electric field. The temporal resolution of the HIBP allows us to observe microsecond time-scale changes of the potential, and gives new information about the electric field transitions. In this Letter, we will describe a dynamic transition in the potential profile observed in the plasma core of the CHS plasma during a combined heating phase of ECH + NBI. We will also present the nonlinear dependence of radial current on radial electric field that causes this bifurcation phenomenon.

The experiments presented here were performed with a magnetic field configuration whose magnitude and axis positions were 0.9 T and 92.1 cm, respectively. The working gas was deuterium and the injected neutral beam was hydrogen. A 300 kW gyrotron of 53.2 GHz was used to produce target plasmas with its resonance position on the magnetic axis. After the pure ECH phase, the NBI with port-through power of 800 kW was also injected into the plasma. Electron temperature profiles were measured with a YAG Thomson scattering system with a repetition rate of 10 ms. The ion temperature profile was obtained with a CXS system. Line averaged electron density was monitored on two chords with HCN interferometers. The observable range of the HIBP covers almost all magnetic flux surfaces [11,12] of this magnetic configuration. The HIBP signal is acquired with a sampling rate of 1 μs. The current amplifier has a frequency band width of 450 kHz. Amplifier noise gives false potential fluctuation with an amplitude of ~20 V in the present experiments. The HIBP has the capability to observe three spatially adjacent points simultaneously using three beam current detectors.

In the ECH heating phase, the central electron temperature is about 800 ± 200 eV, and the line averaged electron density $\overline{n}_e$ is 3×10^{12} cm^{-3}. In the combined heating phase, the electron density gradually increases

 0031-9007/97/79(6)/1054(4)$10.00

from 3×10^{12} cm^{-3} at $t = 50$ ms to 6×10^{12} cm^{-3} at $t = 70$ ms. No significant change in electron temperature was observed with YAG Thomson scattering, while the central ion temperature increases approximately from 100 to 300 eV.

Figure 1 shows the time evolution of potential at several fixed spatial points [1(a)], and potential profiles [1(b)] taken in ECH, ECH + NBI, and NBI phases. A radial scan to obtain a profile took about 9 ms in this case. In the pure ECH phase (A), the potential profile has a sharp peak in the core for $\rho < 0.3$ [open circles in Fig. 1(b)]. Negative ρ in Fig. 1(b) means that the observation point is located below the magnetic axis. As is seen in Fig. 1(a), just after NBI turns on, the central potential increases by 200 V on a time scale of 1 ms, while no significant change is seen at other location. Then the central potential gradually decreases, followed by a sudden drop and rise in the core potential observed at $t = 54.5$ and $t = 56$ ms. On the other hand, the potential near the plasma edge monotonically decreases, and the electric field for $\rho > 0.8$ becomes negative in about 5 ms. In the later period of the combined heating phase (*B*), the potential profile develops into a shape like a "Mexican hat" [closed circles in Fig. 1(b)]; the radial scan is performed from $t = 59$ to $t = 68$ ms. A potential profile similar to this shape has been observed in 100 kW ECH heated plasmas with $\overline{n}_e$ of 8×10^{12} cm^{-3} [14]. After the ECH turns off, the plasma relaxes into the steady state potential profiles [squares in Fig. 1(b)] typical of NBI plasmas in $1 \sim 2$ ms.

Spatial and temporal structure of the drastic change in the core potential, being denoted "transition" in Fig. 1(a), should be examined in more detail. Figure 2(a) demonstrates potential changes at several spatial points, when the observation points are fixed during a shot. The dashed line represents potential profiles taken using a radial scan during an initial phase of ECH + NBI heating as a reference. The data were taken from sequential shots under identical operational conditions. The open squares and closed circles are potential values before and after the transition, respectively [see the arrows in Fig. 2(b)]. In the experimental results we have obtained so far, this dynamic behavior is limited to core radii with $\rho < 0.4$. This figure suggests that the profile changes from sharply peaked to a flat or hollow profile. It is difficult to obtain the fine structural change of profile during the transition, which is happening in a few dozen microseconds. The differences between potential signals from three detectors, which simultaneously observe spatially adjacent points, show to change their signs. These observations imply that the electric field changes from positive to negative. An increase in magnetic field fluctuations was detected at one poloidal position just around the time of the transition, although the causality needs further investigation.

Figure 2(b) shows an expanded view of the rapid rise and drop in the core potential ($\rho = 0$), together with the detected beam current (signal) intensity. The time scale of the potential change can be examined in more detail by fitting a function of $\phi(t, \rho = 0) = 0.5\Delta\phi\{\tanh[(t - t_0)\tau^{-1}] + 1\} + \phi_0$ to the wave form in the transient phase. The fitting parameters for the abrupt drop and rise are $\Delta\phi(\rho = 0) = -179$ V, $\tau = 60$ μs, $t_0 = 54.6$ ms, and $\Delta\phi(\rho = 0) = 395$ V, $\tau = 220$ μs, $t_0 = 56.0$ ms, respectively. The solid lines indicate the fitting curves.

The signal intensity detected with the HIBP exhibits an increase and decrease correlated with the potential drop and rise on a similar time scale. This suggests that the electron density profile is changing in a very local region, especially since no significant change in line averaged density is observed with the interferometer during this rapid change. The signal intensity I_D is expressed as $I_D(r) \propto Q_{12}(r) \exp[-\int_{\text{edge}}^{r} Q_1 \mathrm{d}l_1 - \int_{r}^{\text{edge}} Q_2 \mathrm{d}l_2]$, where $Q_{12}(r)[\propto n_e(r)]$ represents the local ionization rate from the singly charged to the doubly charged state. The exponential term represents the beam attenuation along the beam trajectory, with Q_1 and Q_2 being the total ionization cross sections from the singly charged state

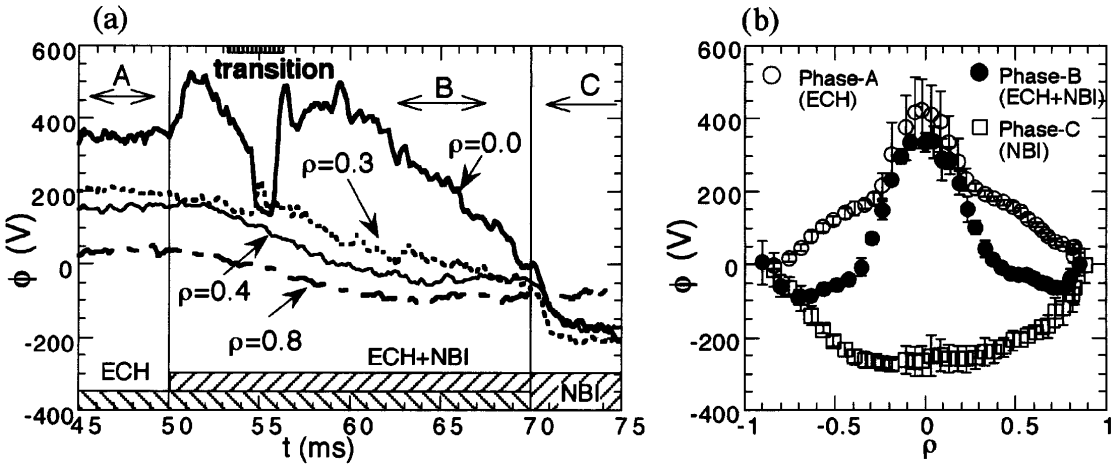

FIG. 1. (a) Time evolution of potential for several spatial points. (b) Potential profiles measured in radial scanning. The open circles, closed circles, and squares represent potential profiles during ECH phase (*A*), combined heating phase of ECH + NBI (*B*), and NBI phase (*C*), respectively.

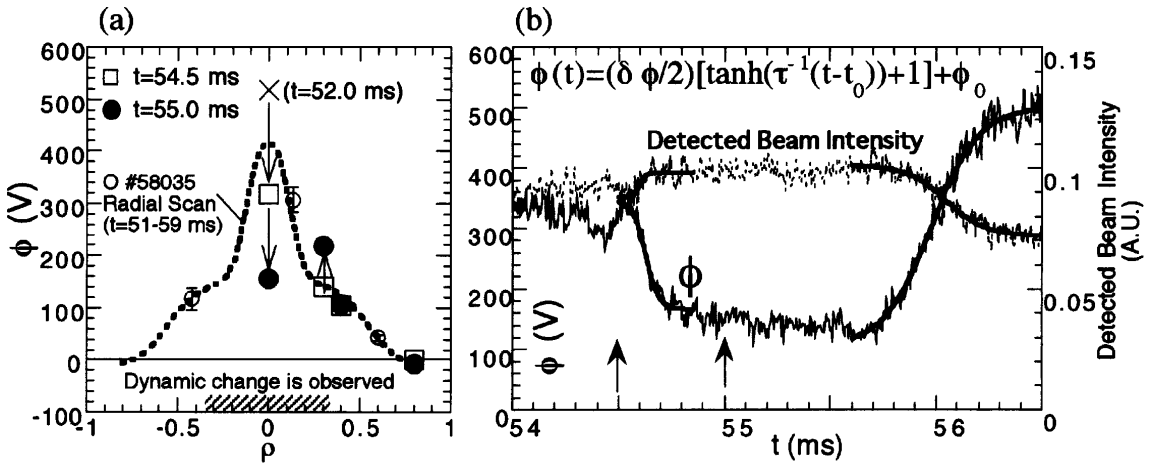

FIG. 2. (a) Potential profile around $t = 54$ ms obtained in scanning mode. The potential changes at several spatial points from $t = 54.5$ to $t = 55$ ms are also shown. (b) Time evolution of $\phi(0)$, and the fitting to the sudden drop and rise, together with time evolution of signal intensity.

and that from the doubly charged state, respectively. The relation of $\Delta Q_{12}/Q_{12} \simeq \Delta n_e/n_e$ indicates the local electron density increases by 15% at $t_0 = 54.6$ ms, and decreases by 30% at $t_0 = 56$ ms, being accompanied with the structural change of the radial electric field. The order of density change is estimated to be $\sim 10^{12}$ cm^{-3}.

The radial electric field change is induced by a radial current, which produces the $j \times B$ force to make the plasma rotate. As a result, the time scale of the transition is connected to the magnitude of the radial current in the following way [5],

$$j_r(E_r) = -\varepsilon_\perp \varepsilon_0 \frac{\partial E_r}{\partial t}, \qquad (1)$$

where $\varepsilon_\perp$ represents the perpendicular dielectric constant of the plasma, with ε_0 being the vacuum dielectric constant. The perpendicular dielectric constant is given by $\varepsilon_\perp = M_{\rm tor}(1 + c^2/v_{\rm A}^2)$, where c and $v_{\rm A}$ are light and Alfvén velocities, respectively. The toroidal enhancement factor is simply estimated as $M_{\rm tor} \simeq 1 + 2q^2$, where q is the safety factor; the q profile of the CHS is approximately expressed as $q = 3.3 - 3.8\rho^2 + 1.5\rho^4 + \ldots$ in a polynomial series.

The radial current change can be estimated by using Eq. (1). We assume that the Alfvén velocity is 8×10^6 m/s, which corresponds to an electron density of $n_e = 3 \times 10^{12}$ cm^{-3}. The perpendicular dielectric constant $\varepsilon_\perp \simeq 2.7 \times 10^4$ when $q \simeq 3$. We will use an average field instead of the local radial electric field in the following analysis, since the exact change of the local electric field is difficult to obtain. The average radial electric field is given by $\overline{E}_r = -[\phi(0.3a) - \phi(0)]/0.3a$.

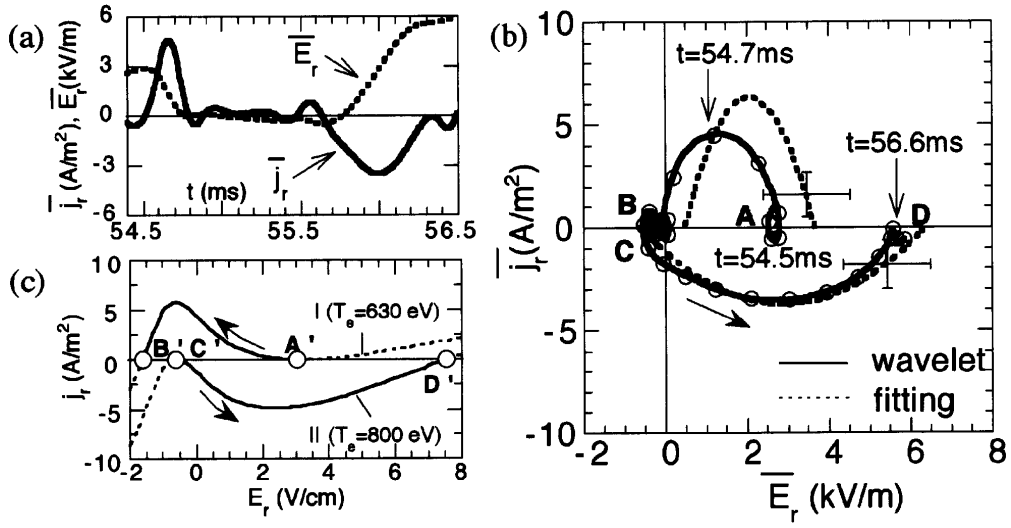

FIG. 3. (a) Experimental radial current to induce electric field change. The solid and dashed lines show the radial current and electric field, respectively. (b) Experimental radial current j_r as a function of radial electric field E_r. The open circles are plotted in every 64 μs. (c) Diagram of calculated radial electric field and radial current using a neoclassical formula. This diagram shows critical conditions to cause transition based on bifurcation.

Using a wavelet analysis on the estimated average electric field, we evaluate the radial current as is shown in Fig. 3(a). The maximum currents are 4.5 ± 3.0 A/m^2 and -3.6 ± 2.4 A/m^2 for the transitions at $t = 54.6$ and $t = 56$ ms, respectively. The error bars in the electric field and radial currents come from the uncertainty in the potential change at $\rho = 0.3$. Figure 3(b) plots the radial current as a function of the radial electric field (*E-J* curve) using wavelet analysis (solid line). The dashed line represents the *E-J* curve obtained from the fitting function in Fig. 2(b). The difference between the curves represents the uncertainty in the fitting functions. These two curves unambiguously demonstrate a nonlinear relationship between the radial current and electric field, which results in the transition of the radial electric field. When the plasma is in the state *A* (or *C*) in Fig. 3(c), a slightly negative (or positive) change in the electric field drives the plasma to move from the original state to another state *B* (or *D*). This is because the induced current is in the direction to increase the change of the electric field.

It is of some interest to compare the observed current with the estimate based on the neoclassical theory [17–19]. The neoclassical contribution could be dominant within various mechanisms to determine the radial electric field for the present experiments [5]. Figure 3(c) indicates two examples of the radial current as a function of radial electric field when the bifurcation condition is satisfied for plausible parameters of the CHS plasma. The expression of fluxes given by Hastings *et al.* [18] is used in this calculation [20]. The temperature and electron density profiles in the calculation are assumed to be all parabolic, with the central values being 350 eV and 5×10^{12} cm^{-3}. The central electron temperature is assumed to be 630 and 800 eV for cases of (I) and (II).

The calculated radial current ~ 5 A/m^2 is within the range of the experimental value. And the topology of the *E-J* curve is identical with the experiment. The width of expected electric field change from state (C') to (D') is larger than that from (A') to (B'). This property of the width is in qualitative agreement with the experiment. The essential conclusion obtained here remains the same if we choose another density profile. With assumption of a flat density profile, the neoclassical estimate of radial current is different from the parabolic case approximately by 50%.

In the CCT and the TEXTOR tokamaks [21,22], an *L-H* mode transition is achieved using biasing electrodes inserted into the plasma edge to produce an electric field. The relationship between applied voltage and induced radial current is obtained, and a gap in the radial current is seen at the electric field where the "forced" transition occurs [22]. In contrast, the *E-J* curve we presented here is obtained for a "spontaneous" transition where no external disturbance exists.

Finally, another interesting discovery is that the potential profile has a sharp peak in the ECH heating phase. The radial electric fields inside and outside of this boundary are estimated to be about 50 and 20 V/cm, respectively, and the corresponding $\mathbf{E} \times \mathbf{B}$ drift velocities are 6 and 2 km/s. The existence of steep gradients in the electric field and velocity at $\rho = 0.3 \sim 0.4$ suggests a momentum transport barrier. The details about this prominent profile feature will be discussed in another article.

In conclusion, we have observed a spontaneous transition in a toroidal helical plasma. During a combined heating phase of ECH + NBI, the steep gradient of potential is destroyed and recovered in 60 and 220 μs by achieving a bifurcation condition. It has been experimentally confirmed for the first time that the *E-J* curve in the toroidal helical plasma has nonlinear characteristics that allow bifurcation in the radial electric field. The radial current governing the time scale of the transition is estimated experimentally to be about 5 A/m^2, which is the same order as neoclassical calculations. The HIBP signals imply that this radial electric field change is accompanied by a local electron density change. We have successfully observed the nature of the spontaneous transition in the radial electric field, and this observation gives new insight into the structural formation of radial electric fields in toroidal plasmas.

[1] F. Wagner *et al.*, Phys. Rev. Lett. **49**, 1408 (1982).
[2] ASDEX Team, Nucl. Fusion **29**, 1959 (1989).
[3] S.-I. Itoh and K. Itoh, Phys. Rev. Lett. **60**, 2276 (1988).
[4] K. C. Shaing and E. Crume, Jr., Phys. Rev. Lett. **63**, 2369 (1989).
[5] For review, e.g., K. Itoh and S.-I. Itoh, Plasma Phys. Control. Fusion **38**, 1 (1996).
[6] D. E. Hastings, R. D. Hazeltine, and P. J. Morrison, Phys. Fluids **29**, 69 (1986).
[7] E. Yahagi, K. Itoh, and M. Wakatani, Plasma Phys. Control. Fusion **30**, 995 (1988).
[8] F. C. Jobes and R. L. Hickok, Nucl. Fusion **10**, 195 (1970).
[9] G. A. Hallock *et al.*, Phys. Rev. Lett. **56**, 1248 (1986).
[10] X. Z. Yang *et al.*, Phys. Fluids B **3**, 3448 (1991).
[11] A. Fujisawa, H. Iguchi, M. Sasao, Y. Hamada, and J. Fujita, Rev. Sci. Instrum. **63**, 3694 (1992).
[12] A. Fujisawa *et al.*, Rev. Sci. Instrum. **67**, 3099 (1996).
[13] K. Matsuoka *et al.*, in *Proceedings of the 12th International Conference on Plasma Physics and Controlled Nuclear Fusion Research, Nice, 1988* (International Atomic Energy Agency, Vienna, 1989), Vol. 2, p. 411.
[14] A. Fujisawa *et al.*, Phys. Plasmas **4**, 1357 (1997).
[15] H. Idei *et al.*, Phys. Rev. Lett. **71**, 2220 (1993).
[16] H. Sanuki *et al.*, Phys. Scr. **52**, 461 (1995).
[17] H. Sanuki, K. Itoh, and S.-I. Itoh, J. Phys. Soc. Jpn. **62**, 123 (1993).
[18] D. E. Hastings, W. A. Houlberg, and K. C. Shaing, Nucl. Fusion **25**, 445 (1985).
[19] L. M. Kovrizhnykh, Nucl. Fusion **24**, 435 (1984).
[20] The calculation here does not include effects of $\partial r^{-1} E_r / \partial r$. The measurements show $\partial r^{-1} E_r / \partial r \simeq 0$ in the core of the plasma [see Figs. 1(a) and 2(a)]. The lines during the transition phase in Fig. 3(c) are also obtained on this assumption.
[21] R. J. Taylor *et al.*, Phys. Rev. Lett. **63**, 2365 (1989).
[22] R. R. Weynants *et al.*, Nucl. Fusion **32**, 837 (1992).